Reduced hexokinase II impairs muscle function 2 weeks after ischemia-reperfusion through increased cell necrosis and fibrosis

Smeele, K.M.; Eerbeek, O.; Schaart, G.; Koeman, A.; Bezemer, R.; Nelson, J.K.; Ince, C.; Nederhof, R.; Boek, M.; Laakso, M.; de Haan, A.; Drost, M.R.; Hollman, M.W.; Zuurbier, C.J.

published in
Journal of Applied Physiology (1985)
2012

DOI (link to publisher)
10.1152/japplphysiol.01494.2011

document version
Publisher's PDF, also known as Version of record

Reduced hexokinase II impairs muscle function 2 wk after ischemia-reperfusion through increased cell necrosis and fibrosis

Kirsten M. Smeele, Otto Eerbeek, Gert Schaart, Anneke Koeman, Rick Bezemer, Jessica K. Nelson, Can Ince, Rianne Nederlof, Maxim Boek, Markku Laakso, Arnold de Haan, Maarten R. Drost, Markus W. Hollmann and Coert J. Zuurbier

J Appl Physiol 113:608-618, 2012. First published 21 June 2012;
doi: 10.1152/japplphysiol.01494.2011

J Appl Physiol 113: 608–618, 2012.
First published June 21, 2012; doi:10.1152/japplphysiol.01494.2011.

Reduced hexokinase II impairs muscle function 2 wk after ischemia-reperfusion through increased cell necrosis and fibrosis

Kirsten M. Smeele,[1] Otto Eerbeek,[2] Gert Schaart,[7] Anneke Koeman,[1] Rick Bezemer,[3] Jessica K. Nelson,[1] Can Ince,[3] Rianne Nederlof,[1] Maxim Boek,[4] Markku Laakso,[5] Arnold de Haan,[6] Maarten R. Drost,[7] Markus W. Hollmann,[1] and Coert J. Zuurbier[1]

[1]*Laboratory of Experimental Intensive Care and Anesthesiology, Department of Anesthesiology;* [2]*Department of Anatomy, Embryology, and Physiology;* [3]*Translational Physiology; and* [4]*Laboratory Genetic Metabolic Diseases, Academic Medical Center, Amsterdam, The Netherlands;* [5]*Department of Medicine, University of Eastern Finland and Kuopio University Hospital, Kuopio, Finland;* [6]*Research Institute MOVE, VU University, Amsterdam, The Netherlands; and* [7]*Department of Human Movement Sciences, NUTRIM School for Nutrition, Toxicology and Metabolism, Maastricht University Medical Centre + (MUMC+), Maastricht, The Netherlands*

Submitted 6 December 2011; accepted in final form 9 June 2012

Smeele KM, Eerbeek O, Schaart G, Koeman A, Bezemer R, Nelson JK, Ince C, Nederlof R, Boek M, Laakso M, de Haan A, Drost MR, Hollmann MW, Zuurbier CJ. Reduced hexokinase II impairs muscle function 2 wk after ischemia-reperfusion through increased cell necrosis and fibrosis. *J Appl Physiol* 113: 608–618, 2012. First published June 21, 2012; doi:10.1152/japplphysiol.01494.2011.—We previously demonstrated that hexokinase (HK) II plays a key role in the pathophysiology of ischemia-reperfusion (I/R) injury of the heart (Smeele et al. *Circ Res* 108: 1165–1169, 2011; Wu et al. *Circ Res* 108: 60–69, 2011). However, it is unknown whether HKII also plays a key role in I/R injury and healing thereafter in skeletal muscle, and if so, through which mechanisms. We used male wild-type (WT) and heterozygous HKII knockout mice ($HKII^{+/-}$) and performed in vivo unilateral skeletal muscle I/R, executed by 90 min hindlimb occlusion using orthodontic rubber bands followed by 1 h, 1 day, or 14 days reperfusion. The contralateral (CON) limb was used as internal control. No difference was observed in muscle glycogen turnover between genotypes at 1 h reperfusion. At 1 day reperfusion, the model resulted in 36% initial cell necrosis in WT gastrocnemius medialis (GM) muscle that was doubled (76% cell necrosis) in the $HKII^{+/-}$ mice. I/R-induced apoptosis (29%) was similar between genotypes. HKII reduction eliminated I/R-induced mitochondrial Bax translocation and oxidative stress at 1 day reperfusion. At 14 days recovery, the tetanic force deficit of the reperfused GM (relative to control GM) was 35% for WT, which was doubled (70%) in $HKII^{+/-}$ mice, mirroring the initial damage observed for these muscles. I/R increased muscle fatigue resistance equally in GM of both genotypes. The number of regenerating fibers in WT muscle (17%) was also approximately doubled in $HKII^{+/-}$ I/R muscle (44%), thus again mirroring the increased cell death in $HKII^{+/-}$ mice at *day 1* and suggesting that HKII does not significantly affect muscle regeneration capacity. Reduced HKII was also associated with doubling of I/R-induced fibrosis. In conclusion, reduced muscle HKII protein content results in impaired muscle functionality during recovery from I/R. The impaired recovery seems to be mainly a result of a greater susceptibility of $HKII^{+/-}$ mice to the initial I/R-induced necrosis (not apoptosis), and not a HKII-related deficiency in muscle regeneration.

fatigue; fibrosis; healing; regeneration; skeletal muscle

SKELETAL MUSCLE ISCHEMIA-REPERFUSION (I/R) frequently occurs in many acute (surgical intervention, circulatory shock, trauma) or chronic (decubitus, diabetes, obstructive vascular disease) clinical situations, resulting in muscle dysfunction and myocyte death, which in turn contributes to increased morbidity and mortality even when limb circulation is restored. Elucidating and subsequent targeting of underlying cellular mechanisms may help alleviate the burden of skeletal muscle I/R. The present study examines a possible role of the glycolytic enzyme hexokinase (HK) II in skeletal muscle I/R injury.

Earlier cellular studies have demonstrated that the glycolytic enzyme HKI or HKII may have strong protective effects against stress-induced cell death (30). In addition, the increased expression of HK in malignant tumors is thought to contribute to the immortalization of cancer cells (25). Recently, we have demonstrated that HKII also plays an important role in the degree of acute injury and remodeling following I/R in the heart (33, 38). In the heart, HKI and HKII are approximate equally distributed. However, in skeletal muscle, HKII is the predominant HK isoform present (34), suggesting an even more prominent role of HKII in skeletal muscle I/R injury compared with the heart. Indeed, we found that reduced HKII resulted in cell death in a noninjurious I/R model of intact mouse skeletal muscle (32). However, in this preliminary study, I/R injury was evaluated after a short period of ischemia (60 min) and reperfusion (90 min) only, resulting in minor I/R injury. Moreover, skeletal muscle has the capacity to regenerate and therefore recover from injury, in contrast to the very limited regenerative capacity of the heart. To our knowledge, no information exists concerning a possible role of HK in severe skeletal muscle I/R injury and regeneration. Therefore, in the present study, an extended period of ischemia (90 min) and prolonged periods of reperfusion (1 day and 14 days) were examined to investigate the effect of HKII on severe muscle I/R injury and subsequent muscle regeneration.

The mechanisms through which HK offers protection are unresolved but probably pertain to its binding to the mitochondria (30, 31, 40). It has been suggested that mitochondrial HK prevents apoptosis through inhibition of mitochondrial binding of the proapoptotic protein Bax (29), although Majewski et al. (24) demonstrated that HK protective effects were still present in Bax-deficient cells. We were also unable to confirm a role for mitochondrial Bax in causing increased I/R injury in HKII-reduced hearts (33). Other mechanisms through which mitochondrial HK may alleviate injury relates to inhibition of necrosis and/or attenuation of oxidative stress through regulation of mitochondrial ATP/ADP exchange (9).

Address for reprint requests and other correspondence: C. J. Zuurbier, Dept. of Anaesthesiology, Academic Medical Center, Univ. of Amsterdam, Meibergdreef 9, 1105 AZ Amsterdam, The Netherlands (e-mail: c.j.zuurbier@amc.uva.nl).

In the present study, we addressed whether HKII reduction affects *1*) acute, severe I/R injury of skeletal muscle, with a possible role for necrosis, apoptosis, glycogen turnover, mitochondrial Bax, and oxidative stress; and *2*) structural and functional healing through regeneration of postischemic, reperfused skeletal muscle tissue. A recently developed, noninvasive approach of the I/R intervention was chosen (7, 26), using orthodontic rubber bands to obtain complete hindlimb ischemia and reperfusion.

METHODS

All procedures were in accordance with the guidelines of and approved by the Animal Ethical Committee of the University of Amsterdam and conform to National Institutes of Health guidelines.

Animals

C57BL/6J mice containing a partial deletion of the HKII gene ($HKII^{+/-}$) (17), were in-house bred under standard housing conditions (12:12-h light-dark cycle; water and food given ad libitum) and fed Purina Laboratory Rodent Diet 5001 standard chow (PURINA; PMI Nutrition International). These animals were shown to have reduced HK activity and HKII isoform levels in both heart and gastrocnemius medialis (GM) skeletal muscle (32, 34), without effect on HKI protein levels. Genotypes were determined by standard PCR technique after extraction of DNA from toe tissue after weaning, and verified from ear tissue analysis after experiment termination. Male mice of 3–4 mo were used.

Experimental Procedures

Prior to performing the actual experiments, we performed pilot experiments in wild-type (WT) animals to determine the amount of injury created with increasing ischemic periods of 1, 1.5, or 2 h followed by 24 h reperfusion (n = 3–5 per group). Injury was determined by the amount of released lactate dehydrogenase (LDH) enzyme from I/R muscle and calculated as the ratio of LDH in the I/R and contralateral control muscle. Subsequently, WT and $HKII^{+/-}$ mice were studied in four different experiments: *group A*, 90 min ischemia followed by 24 h reperfusion (n = 6–8 per group); and *group B*, 90 min ischemia followed by 14 days reperfusion (n = 5–7 per group). Additionally, to examine a possible role of glycogen among the genotypes, glycogen content of GM was determined in two separate groups: *group C*, in I/R GM of WT animals immediately after ischemia (n = 6); and *group D*, in control and I/R GM of WT (n = 6) and $HKII^{+/-}$ animals (n = 9) at 1 h reperfusion following 90 min of unilateral ischemia. For *group D* muscles, caspase-3/7 activity was also determined. At the end of each experiment, all animals were killed using cervical dislocation during a surgical plane of anesthesia.

Validation of ischemia and reperfusion. A laser speckle imaging (LSI) technique was used to assess limb perfusion (6, 11) during ischemia and reperfusion in separate experiments using WT animals (n = 3). For LSI measurements, a commercially available system was used (Moor Instruments). A 785-nm class 1 laser diode was employed for illumination of the tissue, and light directly reflected by the tissue surface was blocked by a tunable polarizer in front of the lens system. Laser speckle images were captured using a 576 × 768 pixels grayscale CCD camera at a frame rate of 25 Hz and converted to pseudo-color images, where the level of perfusion was scaled from blue (low perfusion) to red (high perfusion). I/R was performed in the exact manner and duration as described below. The LSI was positioned ~50 cm above the animal and focused such that both hindlimbs could be monitored simultaneously. Laser speckle images of both GMs were obtained at baseline, ischemia, and reperfusion. The perfusion of the I/R muscle was calculated relative to the perfusion of the contralateral muscle and normalized to baseline values.

Ischemia and reperfusion procedure. In vivo I/R was performed slightly modified from the method described by Crawford et al. (7). Briefly, induction of anesthesia was performed with an intraperitoneal injection of 80 mg/kg pentobarbital sodium and was followed by a subcutaneous injection of 1 ml saline for fluid support. Body temperature of each mouse was monitored continuously with a rectal thermometer and maintained at 37°C throughout the complete procedure using heating pads. Ischemia for 90 min was applied to one hindlimb using two orthodontic rubber bands (no. 110, 3.2 mm, Latex O-Rings; Miltex Instruments) placed together at the most proximal side of the thigh as close to the pelvic as possible using a McGivney Haemorrhoidal Ligator (Miltex Instruments). During ischemia anesthesia was maintained by intraperitoneal injection of 20 mg/kg pentobarbital sodium at 30 min and 75 min after induction. Additionally, 10 mg/kg pentobarbital sodium was injected 100 min after induction (i.e., just before reperfusion) to prevent the mice from moving at the first, crucial minutes of reperfusion. Reperfusion was created by cutting the rubber bands and visually confirmed by the color change of the paw from blue to red. Throughout the I/R procedure the contralateral (CON) hindlimb was left untreated to serve as internal control. Animals returned to the (nonheated) cage after 1 h reperfusion. Animals of experimental *group A* were anesthetized after 1 day reperfusion with ketamine (125 mg/kg), medetomidine (0.2 mg/kg), and atropine (0.5 mg/kg) (41) and GM and gastrocnemius lateralis (GL) of both hindlimbs excised for further analysis. This procedure was also performed for animals of *group B* after 14 days reperfusion with the exception that force measurements (described below) were performed prior to tissue excision.

Force measurements. Preparation and force measurements were identical as previously described (32). In brief, animals were ventilated mechanically after tracheotomy. To perform in situ stimulation, the medial head of the gastrocnemius was prepared free from surrounding tissue, leaving the origin on the femur and blood supply intact. Distally, the Achilles tendon was cut and attached through a metal hook to a force transducer (42). The muscle was stimulated via the severed sciatic nerve, with temperature kept at 37°C throughout the experiment. Muscle optimal length using twitch contractions was determined (10), and maximum twitch and tetanic force was measured. Twitch and tetanic forces were measured as millinewtons and normalized to GM wet muscle mass (Table 1). Both were used as index of functional recovery of I/R relative to CON GM performance. Finally, muscle fatigue was assayed by application of 30 repetitive tetani (stimulation frequency 150 Hz, stimulation duration 50 ms, pulse width 40 μs, one contraction every 250 ms) as described previously (19).

GM cryopreservation and homogenization. CON and I/R GMs from *group A* and *group B* were excised from the anesthetized animals and weighed. Each GM was cut in half over the length-axis. One part was immediately cryopreserved for immunohistological determination by embedding in Tissue-Tek (Sakura Finetek) and quickly frozen

Table 1. *Body weight and GM muscle mass of WT and $HKII^{+/-}$ animals at 1 day reperfusion (n = 8 each group) and 14 days reperfusion (n = 7 each group)*

	WT		$HKII^{+/-}$	
	CON	I/R	CON	I/R
1 Day reperfusion				
Mass, mg	49 ± 3	56 ± 2†	49 ± 2	58 ± 3†
Body weight, g	27.8 ± 0.8		27.4 ± 0.6	
14 Days reperfusion				
GM wet mass, mg	47 ± 2	27 ± 2†	43 ± 2	25 ± 1†
Body weight, g	24.9 ± 0.6		25.1 ± 0.7	

Values are means ± SE. GM, gastrocnemius medialis; WT, wild-type; $HKII^{+/-}$, heterozygous hexokinase II knockout; CON, contralateral control limb; I/R, ischemia-reperfusion. †$P < 0.05$, I/R vs. CON, same genotype.

in liquid nitrogen-prechilled isopentane (Sigma-Aldrich) and directly stored at −80°C until further analysis. The second GM part was directly homogenized in 0.8 ml ice-cold isolation buffer containing (in mM) 250 sucrose, 20 HEPES buffer (pH 7.4), 10 KCl, 1.5 $MgCl_2$, 1 EDTA, 0.1 PMSF, as well as 5 μg/ml leupeptin, 5 μg/ml aprotinin, and 1 μg/ml pepstatin A. Half of the homogenate was centrifuged at 10,000 *g* for 10 min. The pellet contained the crude mitochondrial fraction and the supernatant the cytosolic fraction. The other half of homogenate was determined as whole cell fraction. Samples were directly stored at −80°C until further analysis. Muscles from *groups C* and *D* were excised, immediately frozen in liquid nitrogen, and stored at −80°C until further analysis for glycogen content and caspase-3/7 activity. Mice were subsequently killed by cervical dislocation.

Edema measurement. After excision of GMs, the gastrocnemius lateralis (GL) was excised for *group B*, weighed (to obtain the GL wet weight), and dried in a stove at 60°C for 48 h and weighed again to obtain GL dry weight. Edema was calculated as ratio of wet to dry GL weight.

Postexperimental Analysis

Immunohistochemistry. For the immunofluorescence and the TUNEL-reaction we used 5-μm-thick serial tissue specimens. The specimen from the I/R and CON GM were placed on the same glass slide per experiment. Necrotic cells were detected by intracellular caveolin staining, based on the premise that loss of plasma membrane integrity is a primary characteristic of necrosis. Apoptotic cells were detected by the TUNEL assay (In situ Cell Death Detection Kit, POD, Roche), based on the premise that DNA fragmentation is a primary characteristic of apoptosis (22). For counting the amount of necrotic cells (*group A*, 1 day reperfusion) and analysis of regeneration by measuring cell surface and counting number of cells with centralized nuclei (*group B*, 14 days reperfusion), GM slices were incubated with anti-caveolin (red; CAV; 1:100; BD Biosciences), anti-laminin (green; LAM; 1:50; Sigma), and anti-DAPI (blue; 300 nM; Invitrogen), staining for necrotic cells, cell membrane, and nuclei, respectively. Cells were counted as necrotic when the intracellular surface stained for caveolin. Number of necrotic cells and number of cells with centralized nuclei were counted by hand and analyzed as ratio to the total cell number counted in each picture. The number of apoptotic cells equaled the number of myocyte-related TUNEL-positive nuclei divided by total number of myocyte-related nuclei [= nuclei (DAPI-staining) close to cell membrane (LAM staining)]. Total cell surface was determined by drawing the borders of the laminin-stained cells by hand, hereby eliminating (nonstained) intracellular space, followed by software-determined calculation of the selected area. Subsequently, mean cell surface was determined by dividing total cell surface by total number of cells counted in each picture. Other GM tissue slices were incubated with anti-CD31 (red; 1:100; BD Biosciences) together with anti-laminin (blue; 1:50; Sigma) to stain for capillaries and cell membrane, respectively. Angiogenesis in the GM after 14 days reperfusion was determined by counting the number of CD31-stained capillaries within the LAM-stained myocytes in each image. The number of capillaries was normalized to total cell area, whose borders were drawn by hand, and the area was measured automated and shown as square millimeters. Fibrosis, the amount of intercellular collagen formed, was analyzed by measuring the total collagen surface (red) and total cell surface (pink) in each image after performing a Sirius red staining.

All above-mentioned analyses were performed in a blinded fashion, both to genotype and to condition. Each parameter was determined in three to five images per GM, with each image analyzed two to three times. All images were 20× magnifications, and analysis was performed using Lucia G/F imaging analysis software (Laboratory Imagin, CZ).

Mitochondrial Bax amount. The pellet of the crude mitochondrial fraction from experimental *group A* (1 day reperfusion) was resuspended in isolation buffer and incubated for 1 h with 2% CHAPS to contain Bax oligomers formed due to I/R (1). For tissue lysation the samples were sonicated and debris was removed by centrifugation at 100,000 *g* for 30 min. The supernatant, consisting of the solubilized mitochondrial fraction, was incubated with 1 mM disuccinimidyl suberate (DSS, Thermo Scientific) dissolved in DMSO for cross-linking of Bax complexes. The chemical reaction was stopped by addition of loading buffer containing mercaptoethanol and analyzed for total (monomer and oligomer) mitochondrial Bax amount by Western blotting. Fifteen micrograms of protein per slot was loaded on a 10% SDS-polyacrylamide denaturing gel. PVDF membranes were incubated with anti-Bax (1:1,000; BD Biosciences) and anti-VDAC (1:10,000; Calbiochem) as loading control, followed by horseradish peroxidase-conjugated secondary goat anti-mouse antibodies (1:10,000; Jackson ImmunoResearch) and anti-biotin (1:2,000; Cell Signaling). Immunoreactive bands were visualized by chemiluminescence on X-ray film (Hyperfilm ECL, Amersham) using enhanced chemiluminescence solution (Santa Cruz). For quantification a Kodak Image Station 440CF (Eastman Kodak) was used. Each sample was analyzed in duplicate.

Oxidative stress. Homogenized I/R and CON GM tissue samples of experimental *group A* (1 day reperfusion) were analyzed. Oxidative stress was determined by analyzing the degree of protein carbonylation in the supernatant of whole cell homogenate, obtained after 0.5% Triton X-100 treatment and centrifugation at 12,000 *g* for 10 min. The method uses derivatization of protein carbonyl groups with 2,4-dinitrophenyl hydrazine (DNPH) producing hydrazone, which is detected spectrophotometrically (Protein Carbonyl Assay kit; Cayman Chemical). Values were normalized to sample protein concentration (Bradford assay).

Enzyme activity measurements. GM whole cell homogenate of experimental *group B* was treated with 0.5% Triton X-100 to solubilize hexokinase (21), followed by centrifugation (12,000 *g*; 1 min) to pellet crude undissolved remnants. All enzyme activities were spectrophotometrically determined in the resulting supernatant at 25°C. HK and citrate synthase (CS) activity was measured as reported previously (16). HK activity was normalized to CS activity. Lactate dehydrogenase (LDH), as index of necrosis used in the pilot experiments, was measured using KH_2PO_4 buffer, NADH, and pyruvate and normalized to sample protein (Bradford assay) concentration.

Glycogen amount. Frozen muscles were grinded into powder in liquid nitrogen, and a small part of the powder was used for glycogen determination, the other part for caspase 3/7 activity analysis. Glycogen was enzymatically converted to glucose using amyloglucosidase (Roche Diagnostics). Glucose was determined by a two-step enzymatic method using HK and glucose-6-phosphate dehydrogenase (both Roche Diagnostics) as described in Ref. 3. Liquid handling was performed by a Freedom EVO 100 robot (Tecan) and formation of NADPH was measured fluorometrically using an Infinite plate reader (Tecan). Values were normalized to sample protein concentration (Bradford assay).

Caspase-3/7 activity assay. Part of the grinded GM was dissolved in 0.6 ml ice-cold isolation buffer containing (in mM) 250 sucrose, 20 HEPES buffer (pH 7.4), 10 KCl, 1.5 MgCl2, 1 EDTA, 0.1 PMSF, as well as 5 μg/ml leupeptin, 5 μg/ml aprotinin, 1 μg/ml pepstatin A, and 0.5% CHAPS (Sigma-Aldrich). After 5 min incubation at room temperature, each sample was sonicated for 5 s and subsequently centrifuged at 12,000 *g* for 10 min at 4°C. The supernatant was transferred into a new vial and stored at −80°C until further analysis. Caspase-3/7 activity was assessed in the supernatant with the Caspase-Glo 3/7 assay kit (G8090, Promega, Madison, WI). Seventy-five microliters of supernatant was diluted in 75-μl assay buffer, and luminescence was detected according to the manufacturer's protocol. Values were normalized to sample protein concentration (Bradford).

Statistics

Values are presented as means ± SE. Differences between WT and $HKII^{+/-}$ groups were analyzed by a two-way ANOVA (main effects: genotype and I/R treatment; interaction effect: genotype × I/R-treatment) for repeated measurements followed by contrast compari-

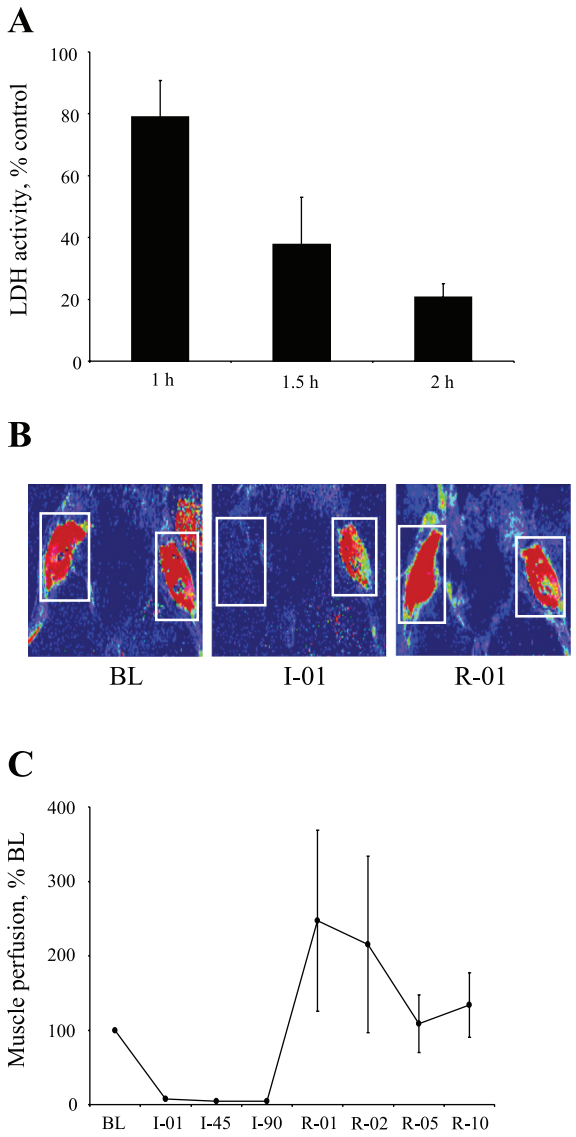

Fig. 1. Model characterization measurements. *A*: cytosolic lactate dehydrogenase (LDH) activity measurements as parameter for cellular injury, shown as percentage of ischemia-reperfusion (I/R) compared with contralateral (CON) limb values as measured in pilot experiments with 1, 1.5, or 2 h ischemia followed by 1 day reperfusion. Muscle perfusion was measured using using laser speckle imaging. *B*: images of the same mouse of both hindlimbs at the moment of baseline (BL), 1 min ischemia (I-01), and 1 min reperfusion (R-01). Left limb is I/R and right limb is CON limb. Degree of perfusion is visualized by color: blue = none to low, yellow = medium, and red = high perfusion. *C*: muscle perfusion during I/R ($n = 3$), normalized to CON limb and relative to BL values. Values are given as means ± SE.

son (SPSS version 18). Differences were considered statistically significant at $P < 0.05$.

RESULTS

Model Characteristics

Optimalization of ischemic model. The degree of I/R damage is critically dependent on the duration of ischemia. Therefore, we performed pilot experiments to determine the optimal duration of ischemia at which damage would be severe enough, but still be amenable to decreases or increases. Ischemia was applied for 1, 1.5, or 2 h and followed by 24 h reperfusion. LDH measurements, as parameter of necrosis and therefore muscle damage, showed that with each 30-min prolongation of ischemia the degree of damage was increased proportionally (Fig. 1*A*). The optimal duration of ischemia to test our hypotheses appeared to be 90 min, resulting in ~60% muscle damage as measured by LDH leakage from the I/R GM muscle.

Muscle perfusion. To validate successful ischemia and reperfusion in this noninvasive I/R model, we monitored relative muscle perfusion simultaneously in both hindlimbs using laser speckle imaging. Figure 1*B* (middle panel) clearly shows immediate, near-complete occlusion of limb perfusion upon tight application of two rubber bands. Removal of the occlusion immediately restored blood flow in the whole limb (Fig. 1*B*, right panel). Applying I/R to one hindlimb appeared to be without influence on muscle perfusion in the contralateral, control hindlimb (Fig. 1*B*). Hyperemia was clearly detectable during the first minutes of reperfusion, after which perfusion returned close to normal from 5 min reperfusion onward (Fig. 1*C*).

Thus the method of I/R application that was used appeared to be nondamaging to the limb vasculature and resulted in severe ischemic injury when applied for 90 min and successful reperfusion of the hindlimb in vivo.

One Hour Reperfusion

Glycogen content. No differences were observed between glycogen content in control muscles between genotypes (Fig. 2*A*).

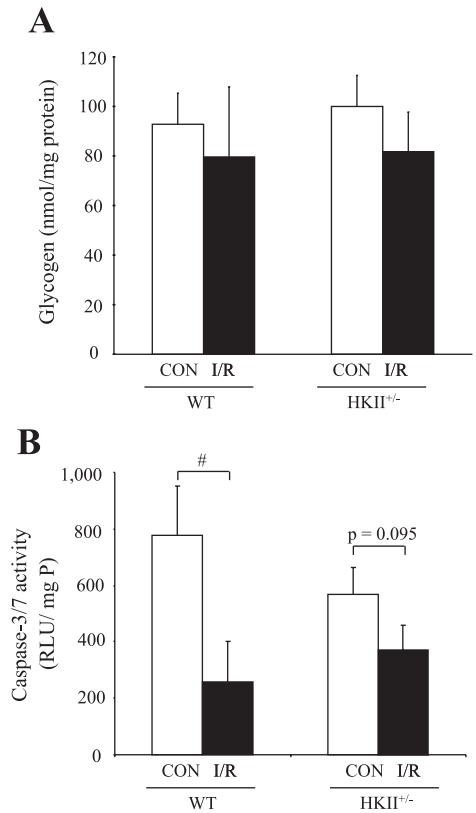

Fig. 2. Glycogen content and caspase-3/7 activity after ischemia followed by 1 h reperfusion. Glycogen was measured in control and I/R muscle tissue of wild-type (WT) and heterozygous hexokinase II knockout ($HKII^{+/-}$) mice (*A*). Caspase-3/7 activity was determined in control and I/R muscle tissue of WT and $HKII^{+/-}$ mice (*B*). Values are given as means ± SE. #$P < 0.05$ vs. CON group of same genotype.

At 1 h reperfusion, there was a clear trend of diminished glycogen content in I/R muscles relative to control muscles, indicating glycogen breakdown during the ischemic period. However, no differences in I/R-induced glycogen breakdown between genotypes were detected. In a second series of experiments we measured glycogen content in I/R wild-type muscle immediately after ischemia, thus without reperfusion. The measured amount of glycogen (17.4 ± 3.2 nmol/mg protein) in ischemia-only muscle is much lower than the glycogen content of 1 h reperfused muscles (79.7 ± 28 nmol/mg protein), indicating that 1 h reperfusion does substantially recover muscle glycogen content.

Caspase-3/7 activity. Caspase activity was measured in control and I/R muscle of both genotypes at 1 h reperfusion (Fig. 2*B*). No differences in caspase activity in control muscles between WT and HKII$^{+/-}$ mice were detected. Surprisingly, caspase activity in I/R muscle of WT was significantly decreased compared with control muscle. However, no differences in I/R-induced alterations in muscle caspase activity between WT and HKII$^{+/-}$ mice were observed.

Twenty-Four Hours Reperfusion

Cellular damage. I/R-induced muscle necrosis and apoptosis were clearly present after 24 h reperfusion, as assessed using histological analysis. As the representative images in Fig. 3*A* show, CON myocytes of both genotypes were unaffected by the I/R procedure performed with the opposite limb as they had retained their normal morphological features—polygonal shape and tightly aligned—and did not stain intracellularly for caveolin. In I/R GM of WT animals 36% of myocytes were necrotic (Fig.

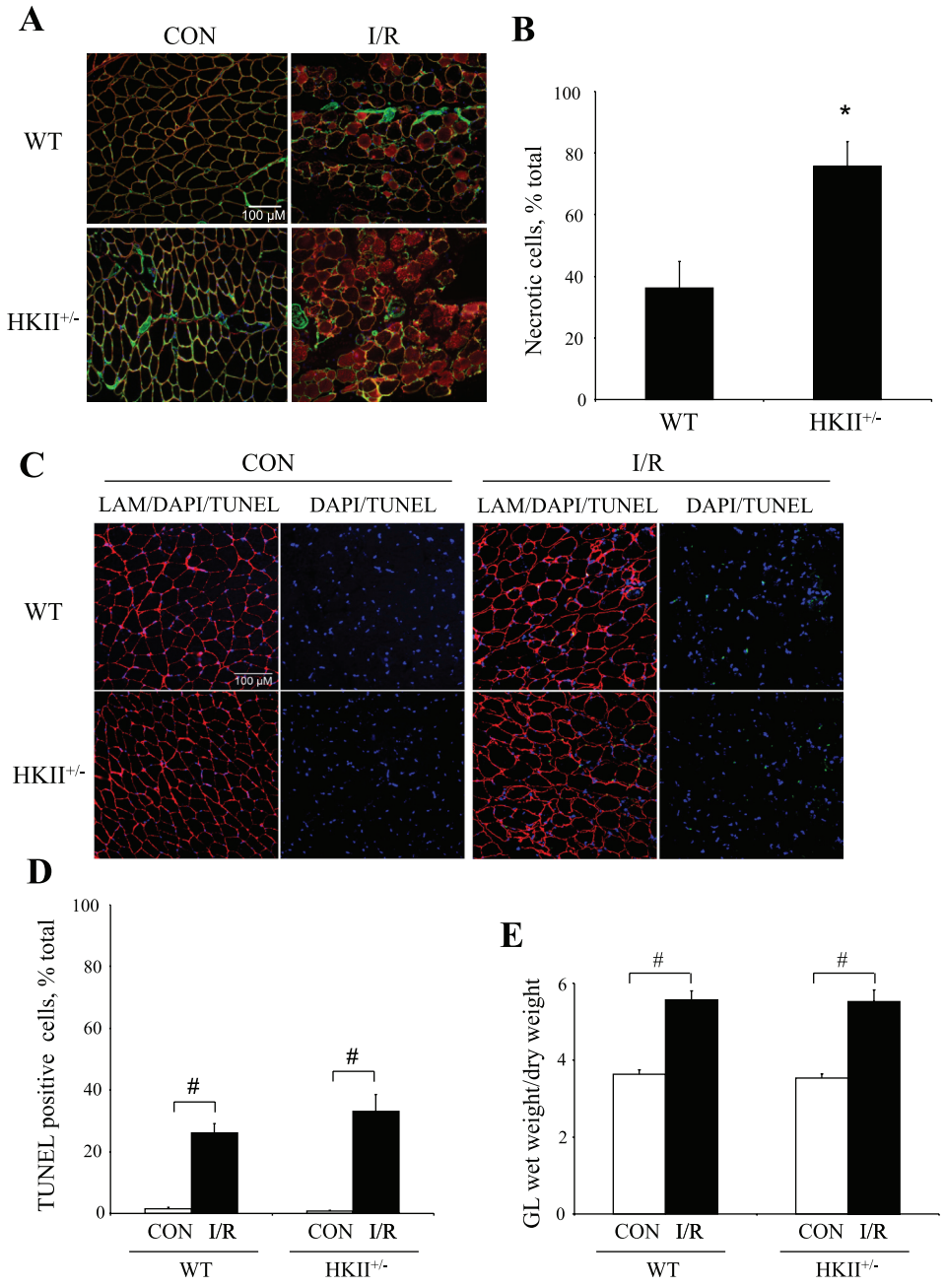

Fig. 3. Tissue damage after ischemia followed by 1 day reperfusion. Cellular necrosis and apoptosis were histologically evaluated using caveolin (red; CAV), laminin (green; LAM), and DAPI (blue) for necrosis (*A*) and using laminin (red; LAM), DAPI (blue), and TUNEL (green) for apoptosis (*C*) staining, respectively. The number of necrotic cells (*B*) and apoptotic cells (*D*) are shown relative to total cell count in each image. Increased edema (*E*) was found in I/R muscle tissue compared with CON as measured by gastrocnemius lateralis (GL) wet-to-dry weight ratio. Values are given as means ± SE. *$P < 0.05$ vs. WT group. #$P < 0.05$ vs. CON group of same genotype.

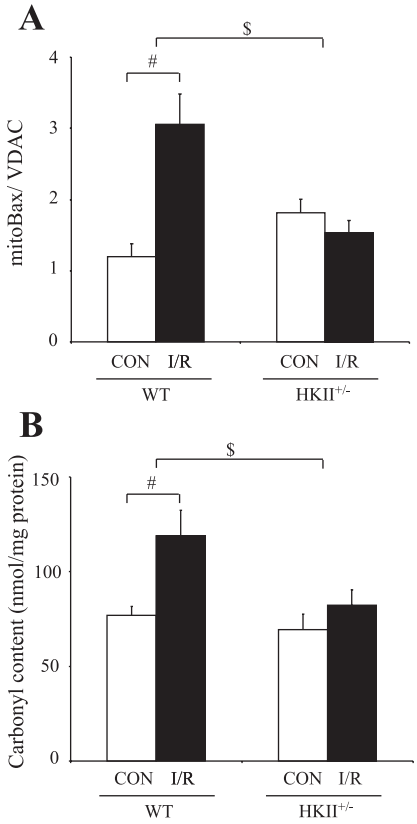

Fig. 4. Proapoptotic Bax and oxidative stress were investigated at 1 day reperfusion. *A*: mitochondrial Bax normalized to VDAC content of I/R and CON GM muscles of WT and HKII$^{+/-}$. *B*: protein carbonylation content of WT and HKII$^{+/-}$ GM and shown as carbonyl content normalized to protein content. Values are given as means ± SE. #$P < 0.05$ vs. corresponding CON group. \$$P < 0.05$ for interaction effect (I/R treatment effect in WT vs. that in HKII$^{+/-}$).

3*B*) and were morphologically mostly rounded and separated from each other (Fig. 3*A*). The number of necrotic myocytes was significantly increased to 76% in HKII$^{+/-}$ animals (Fig. 3*B*). Apoptotic cells were barely detectable in control muscle of both genotypes (Fig. 3, *C* and *D*). I/R induced an increase in apoptotic cells to 26 ± 3% (WT) and 33 ± 6% (HKII$^{+/-}$) muscle. However, the I/R-induced increase in apoptosis was not significantly different between WT and HKII$^{+/-}$ muscle. I/R-induced edema was ~50% for both WT and HKII$^{+/-}$ animals (Fig. 3*E*).

I/R-induced mitochondrial Bax and oxidative stress. Since HKII may exert its cellular protective role by directly influencing the amount of mitochondrial bound proapoptotic protein Bax, due to competition for the same mitochondrial binding site (29), we investigated the total amount of mitochondrial Bax (Fig. 4*A*). Mitochondrial Bax more than doubled in WT animals upon I/R, indicating that skeletal muscle I/R is indeed associated with a translocation of Bax to mitochondria. Remarkably, this effect of I/R on mitochondrial Bax was absent in HKII$^{+/-}$ animals. No differences were observed in amount of mitochondrial Bax in CON GM between WT and HKII$^{+/-}$ animals.

To study a possible effect of HKII on oxidative stress due to I/R, the degree of protein carbonylation in the whole cell homogenate of the GM was studied. As Fig. 4*B* shows, increases in protein carbonylation in the I/R muscle were observed for WT animals, indicating that skeletal muscle I/R is indeed associated with elevated oxidative stress. Surprisingly, I/R was not associated with increased carbonylation in the GM of the HKII$^{+/-}$, whereas basal levels of carbonylation in the CON muscle were similar between genotypes. The data therefore indicate that the increased injury following I/R in the HKII$^{+/-}$ muscle cannot be explained through increases in mitochondrial Bax or oxidative stress.

Fourteen Days Reperfusion

As a result of the finding that HKII reduction does severely increase the amount of cells injured due to the I/R procedure, we investigated whether HKII reduction would also influence the subsequent muscle repair processes. GM tissue was studied after 90 min ischemia and a subsequent period of 14 days reperfusion, a moment at which all injured cells have been eliminated and different processes of skeletal muscle regeneration are in progress (20, 27).

Mitochondrial capacity and HK activity. To examine whether I/R and regeneration affected mitochondrial capacity and total HK activity relative to mitochondrial content, and to what extent this was affected by the deletion of one HKII allele, CS and HK activity were determined. CS was not different between genotypes and was unaffected by I/R and regeneration (Fig. 5*A*). Contrastingly, I/R and regeneration resulted in large increases in HK activity relative to CS activity. This increase was unaffected by

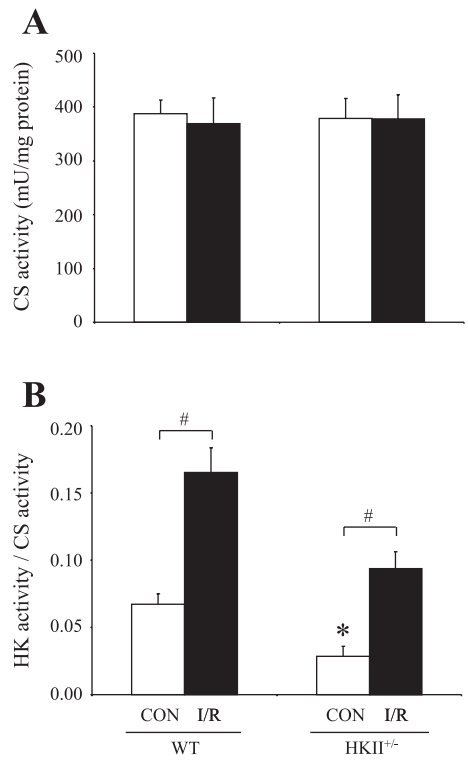

Fig. 5. Mitochondrial capacity and HK activity measured in WT and HKII$^{+/-}$ whole cell homogenate of ischemia-reperfusion treated (I/R) and contralateral (CON) GM after 14 days reperfusion. *A*: citrate synthase (CS) activity values normalized to protein content as parameter of mitochondrial capacity. *B*: HK activity shown as ratio to CS enzyme activity. Values are given as means ± SE. *$P < 0.05$ vs. corresponding WT group. #$P < 0.05$ vs. CON group of same genotype.

the ablation of one HKII allele (Fig. 5*B*). The data indicate that the response of skeletal muscle to a severe ischemic period followed by 14 days of healing contains a large increase of the HK enzyme without alterations in mitochondrial capacity. Ablation of one HKII allele resulted in ~50% reduction in total HK activity compared with WT, indicating that HK activity in GM is predominantly HKII activity.

Functional recovery and fatigue resistance. Both twitch (8.2 ± 0.6 vs. 10.4 ± 0.6 mN/mg) and tetanic force production (31.5 ± 2.1 vs. 34.0 ± 2.0 mN/mg) were similar for control GM between WT and $HKII^{+/-}$ mice, respectively. However, HKII reduction diminished both twitch (Fig. 6*A*) and tetanus (Fig. 6*B*) force recovery following ischemia and 14 days healing: functional recovery in $HKII^{+/-}$ GM was ~50% of the recovery observed for WT GM. Resistance to fatigue was investigated by measuring the developed force upon application of 30 repetitive tetani and relating the value measured for each tetanus to the value of the first tetanus during reperfusion (Fig. 6*C*). The high-intensity fatigue protocol showed a strong decrease in force in the control GM, which was not significantly different between WT and $HKII^{+/-}$. I/R and 14 days healing resulted in increased fatigue resistance of the GM of both genotypes. The I/R-induced increase in fatigue resistance was not affected by ablation of one HKII allele.

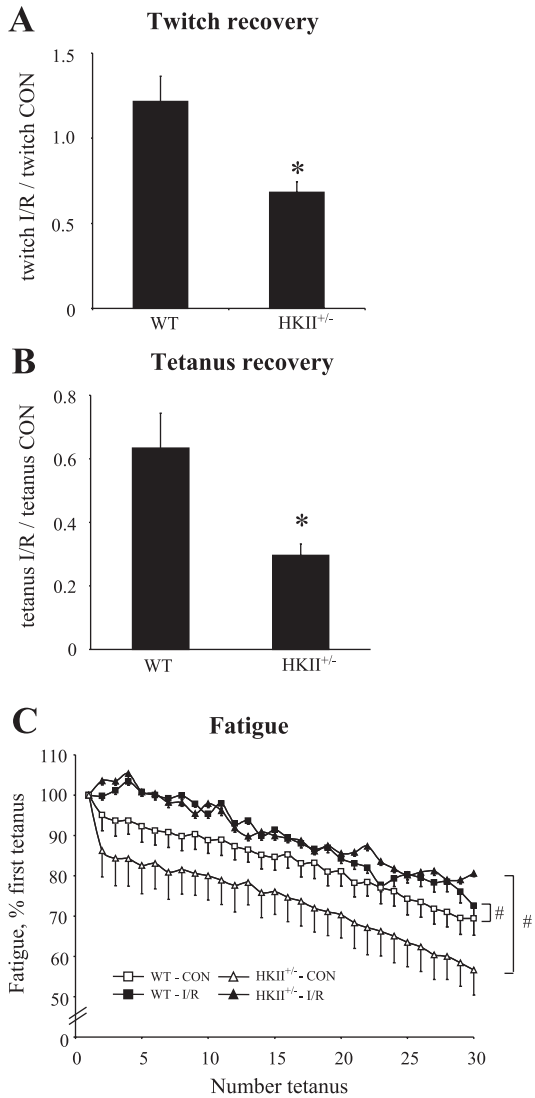

Fig. 6. Functional recovery of GM after ischemia and 14 days reperfusion. Twitch (*A*) and tetanus (*B*) recovery shown as ratio of I/R to CON GM values. *C*: muscle fatigue as tested by applying 30 repetitive tetani. Developed force at each tetanus for both CON and I/R GM was measured and shown as ratio to first tetanus of same group. Values are given as means ± SE. #$P < 0.05$ vs. CON group of same genotype.

Muscle regeneration. Muscle regeneration is characterized by the presence of immature fibers recognized as centronucleated fibers of small size. Representative images in Fig. 7*A* clearly demonstrate the smaller (−52 to −55%) cell size and increased incidence of centronucleated cells following I/R for both WT and $HKII^{+/-}$ mice. No centronucleated myocytes were found in CON muscles of both genotypes. Surprisingly, cell size in the $HKII^{+/-}$ CON muscle was significantly smaller (−14%) than that in the WT CON muscle (Fig. 7*B*), indicating that HKII may be a determinant of myocyte cell size. I/R reduced cell size to a large extent in our model; the reduction was not different between WT and $HKII^{+/-}$ mice. In contrast, the number of centronucleated fibers in the I/R muscle was significantly larger for $HKII^{+/-}$ GM (44%) compared with that in the WT GM (17%; Fig. 7*C*).

Angiogenesis. Capillaries were detected using the endothelial marker CD31 (Fig. 8*A*). No significant differences were observed in capillary density of CON muscle between WT and $HKII^{+/-}$ mice. I/R and 14 days healing resulted in increased capillary density of the GM; this increase, however, was not affected by the partial deletion of the HKII allele (Fig. 8*B*). The data indicate therefore that HKII does not play a critical role in skeletal muscle angiogenesis following I/R.

Fibrosis. The degree of fibrosis that developed in reaction to the I/R intervention was investigated by measuring the amount of interstitial collagen. In both Fig. 9*A* (representative images) and 9*B*, it is shown that fibrosis amounted to 1.3% and 0.9% of muscle area in control GM of WT and $HKII^{+/-}$ mice, respectively. I/R increased fibrosis to 4.5% in WT mice and to 6.8% in $HKII^{+/-}$ mice; the increase in the $HKII^{+/-}$ mice was significantly larger compared with that in the WT mice. The almost doubling of I/R-induced fibrosis at 14 days healing in the $HKII^{+/-}$ mice mirrors the doubling of acute I/R-induced cell necrosis in these muscles (Fig. 3*B*). This indicates that HKII probably does not play a major role in the development of fibrosis during muscle healing.

DISCUSSION

The major findings of this study are that reductions in HKII in a skeletal muscle model of I/R result in *1*) increased myocyte cell necrosis at *day 1* of reperfusion, without alterations in I/R-induced glycogen turnover or apoptosis or increases in mitochondrial Bax and oxidative stress; *2*) reduced functional recovery; and *3*) increased fibrosis without affecting I/R-induced angiogenesis at *day 14* of reperfusion. The observation that the doubling of acute I/R injury at *day 1* translates directly into a doubling of the number of regenerating fibers and a doubling of fibrosis at *day 14* indicates that HKII mainly affects the acute I/R intervention and not the subsequent regeneration capacity of skeletal muscle.

HKII and Acute I/R Cell Damage

We observed ~40% injured GM fibers following 90 min ischemia and 24 h reperfusion, values that fall within the

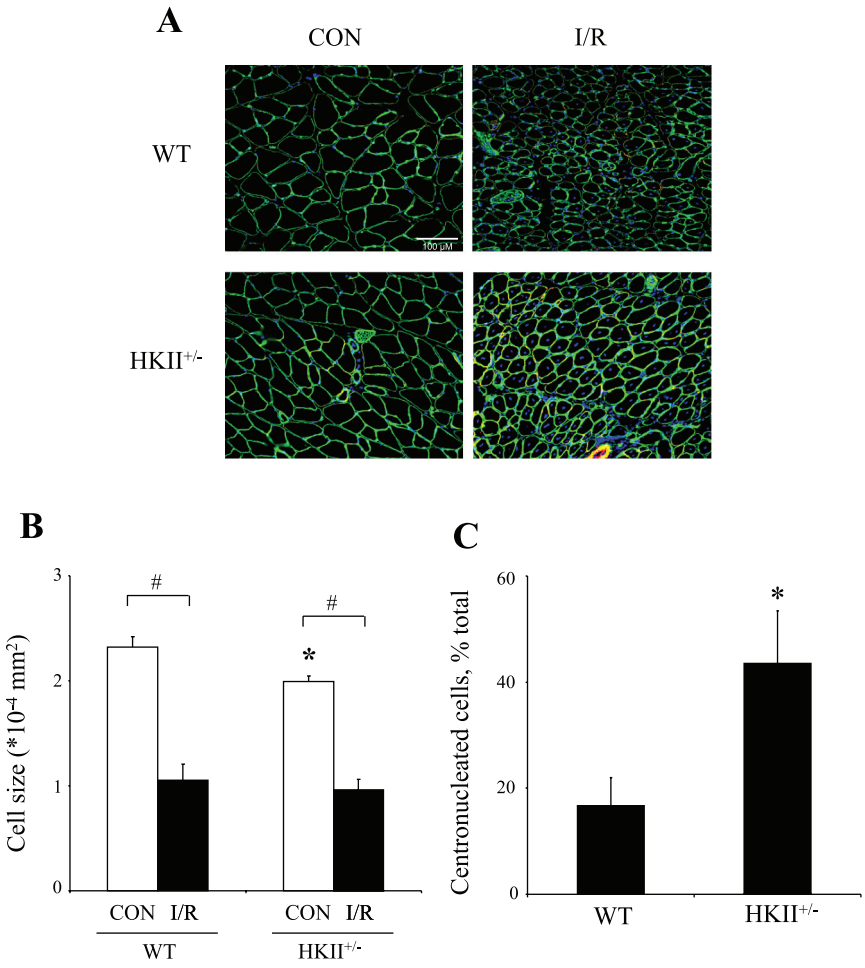

Fig. 7. Muscle regeneration after ischemia followed by 14 days reperfusion. Cell plasma membranes were stained by laminin (green) and nuclei were stained by DAPI (blue). *A*: representative pictures of CON and I/R GM tissue of WT and HKII$^{+/-}$ animals with both stainings shown in each image. Mature myocytes are recognized by nuclei at the border of each cell and polygonal shape, while immature myocytes are recognized by nuclei in the center of the cell, the rounded shape, and smaller size. *B*: average cell size was measured in both CON and I/R GM. *C*: the number of cells with centralized nuclei relative to the total number of cells was counted in GM of WT and HKII$^{+/-}$ animals. Values are given as means ± SE. *$P < 0.05$ vs. corresponding WT group. #$P < 0.01$ vs. CON group of same genotype.

reported range of 30–60% GM injury following 90–120 min ischemia and 24 h reperfusion (5, 26, 39). In a previous study in skeletal muscle, we showed that noninjurious I/R for WT muscle became mildly injurious with reductions in HKII (32). The present work underscores the importance of HKII in injurious I/R of skeletal muscle. In heart, we recently showed that upon 25% reduction of cardiac HKII, I/R injury was increased by 60% (38). In the present study, skeletal muscle HKII content was decreased by 40% (34), and I/R injury was increased by 109%. Even though obtained in different tissues, these results imply that the amount of HKII is inversely related to the degree of I/R injury and therefore emphasize the importance of HKII protein levels in relation to acute skeletal muscle cell survival.

In the past, mitochondrially bound HK was found to be the key factor in reducing apoptosis through inhibition of the mitochondrial permeability transition pore (mPTP) opening. The proposed mechanism was that HK prevented proapoptotic Bax binding to the mitochondrion by direct competition for the same mitochondrial binding site (29). However, the importance of Bax in the process of I/R damage and thereby HKII cellular protection is under debate since Majewski et al. (24) showed that HKII protection was found with and without Bax present. Very recently, we did not find Bax-mediated apoptotic pathway to be involved in mitochondrial HKII dissociation-mediated I/R injury in the intact heart (33). The present results support our previous work and that of Majewski et al. (24) in that mitochondrial Bax is probably not the mediator through which reductions in total cellular HKII result in increased I/R cell death in muscle. Moreover, our results clearly indicate that HKII content mainly affects the necrotic pathway of cell death in a model of in vivo skeletal muscle I/R. No changes in apoptotic cells or caspase activity were observed with reduced skeletal muscle HKII content. It should be realized that necrotic and apoptotic pathways of cell death are not completely separate entities; they are often interconnected (22). Although not directly examined in the present study, it is possible that the decreased caspase activity in the I/R muscle of WT mice at 1 h reperfusion is a consequence of disruption of the plasma membrane (= necrosis) and therefore leakage of the caspase protein out of the myocyte. This could be one example as to how necrosis may affect the apoptotic machinery. In addition, increases in oxidative stress have also been proposed to mediate the increased I/R-induced cell death with decreases in mitochondrial HK (9, 28). In our experimental model, I/R was indeed associated with increases in oxidative stress in WT animals. Surprisingly, this increase in oxidative stress was significantly attenuated in the HKII$^{+/-}$ mice, making it unlikely that increases in oxidative stress may explain the increased cell death with chronic decreases in HKII. We previously demonstrated that mitochondrial HKII is needed to keep mitochondria polarized (33). It is possible that in the HKIII$^{+/-}$

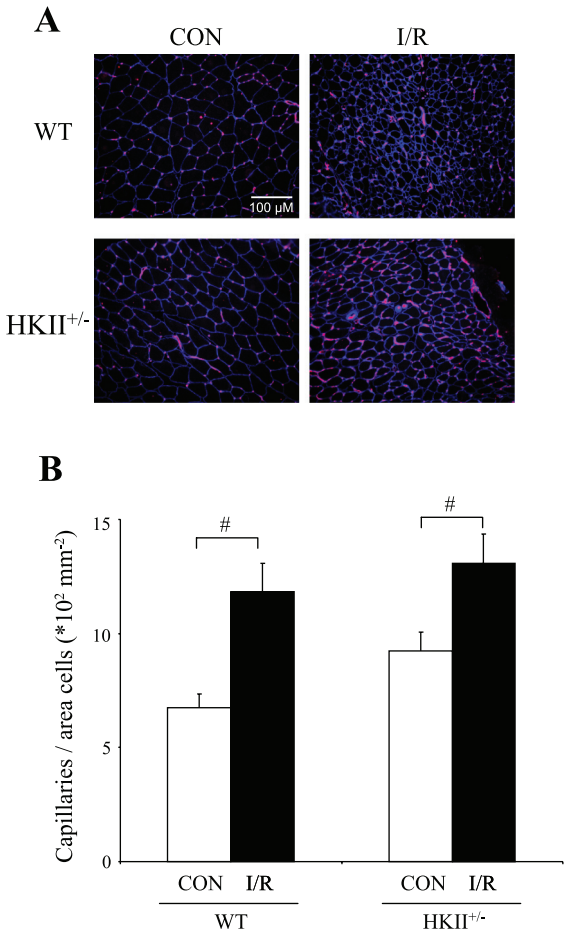

Fig. 8. Angiogenesis in skeletal muscle after ischemia followed by 14 days reperfusion. Capillaries were visualized by CD31 staining (pink) and plasma membranes were stained by laminin (blue). *A*: representative pictures of CON and I/R GM tissue of WT and HKII$^{+/-}$ animals with both stainings shown in each image. *B*: number of capillaries was measured and normalized to the total area of cells in each image in CON and I/R GM of WT and HKII$^{+/-}$ animals. Values are given as means ± SE. #$P < 0.01$ vs. CON group of same genotype.

mice, the reduction in mitochondrial HKII results in an increased number of depolarized mitochondria, normally occurring during I/R (23), which is directly translated into increased I/R damage.

Alternatively, alterations in glycogen turnover during I/R may also partly explain the increased injury, although the amount of glycogen in relation to I/R damage is often a double-edged sword as shown by Cross et al. (8). High glycogen may protect against damage as long as it is not depleted. With lasting ischemia and consequently full depletion of initial high glycogen, a high glycogen actually may result in increased I/R damage. Our results clearly indicate that the observed increase in necrosis with reductions in HKII cannot be explained by alterations in glycogen turnover.

Although further experiments are needed to elucidate the mechanism through which chronic reductions in HKII exacerbate skeletal muscle I/R-induced myocyte necrosis, the present work discards a possible role for glycogen turnover or apoptosis in explaining increased injury with reductions in HKII in a model of in vivo skeletal muscle I/R.

HKII and Skeletal Muscle Recovery After I/R

The present study clearly demonstrates reduced functional recovery and increased fibrosis in skeletal muscle of HKII$^{+/-}$ mice at 14 days recovery following I/R injury. This observation can be explained by *1*) a HKII-related deficiency in muscle regeneration following I/R injury, and/or *2*) a greater susceptibility of HKII$^{+/-}$ mice to the initial damage of I/R. In general, HKII is increased in highly proliferating, growing tissues (25) to support the increase in biosynthetic activity in such tissues. Our observations that HKII is increased in regenerating I/R muscles and that skeletal muscle cell size in control muscle is smaller in the HKII$^{+/-}$ mice are commensurate with this role of HKII in growth and proliferation. However, the finding of an increased number of regenerating muscle fibers in the GM of HKII$^{+/-}$ mice compared with WT mice suggests that reductions in HKII do not result in reduced regeneration. The similar weight of the reperfused GM muscle for both WT and HKII$^{+/-}$ mice at 14 days recovery also indicates that muscle regeneration is not reduced by reductions in HKII. Actually, the observation that the doubling in the number of

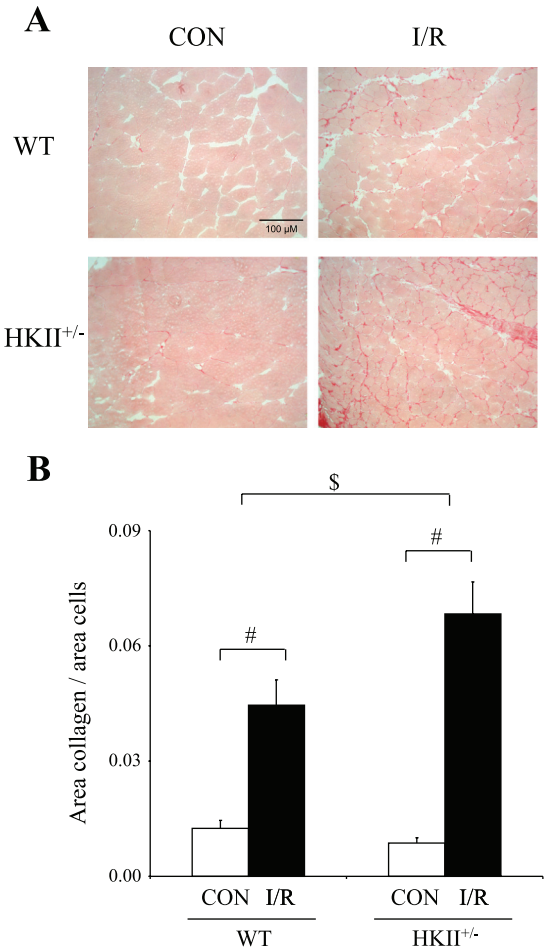

Fig. 9. Fibrosis in skeletal muscle after ischemia followed by 14 days reperfusion. *A*: representative pictures (*A*) showing Sirius red staining for collagen (red) and muscle tissue (pink) of CON and I/R GM tissue of WT and HKII$^{+/-}$ animals. *B*: total area of collagen was normalized to the total area of cells in each image for I/R and CON GM of WT and HKII$^{+/-}$ animals. Values are given as means ± SE. #$P < 0.01$ vs. CON group of same genotype. \$$P <$ 0.05 for interaction effect (I/R treatment effect in WT vs. that in HKII$^{+/-}$).

regenerating fibers in $HKII^{+/-}$ muscle at 14 days recovery mirrors the doubling in number of death of fibers in $HKII^{+/-}$ muscle at 1 day reperfusion indicates that the regeneration process is not directly affected by HKII. Our data therefore suggest that the reduced recovery of GM in $HKII^{+/-}$ mice is mainly a result of a greater susceptibility of $HKII^{+/-}$ mice to the initial damage of the I/R insult, and not to a deficiency in muscle regeneration. The increased fibrosis with reductions in HKII also probably reflects the increased initial I/R damage in these mice and is in agreement with the increased cardiac fibrosis observed using the same mouse model following an in vivo cardiac I/R insult (38).

The increase in capillary density at 14 days recovery is similar to previous findings of increased capillarization following I/R in skeletal muscle (18, 35). That the I/R-induced increase in capillary density was similar for $HKII^{+/-}$ and WT muscle indicates that HKII does not affect I/R-induced angiogenesis. In a previous study using the same mouse model, we observed decreased capillary density in the border zone of the I/R-subjected heart, and the decrease was exacerbated in the $HKII^{+/-}$ mice (38). However, this discrepancy is very likely caused by the fact that the heart has very limited regenerating capacity, such that the decreased capillary density observed for the reperfused heart is mainly a consequence of cell death and fibrosis in the border zone, which were both increased for $HKII^{+/-}$ mice compared with WT mice.

Functional recovery. The tetanic force deficit following 14 days recovery is approximately 35% for WT mice and 70% for $HKII^{+/-}$ mice, again mirroring the initial damage observed in each genotype (cell death of 36% and 76% for WT and $HKII^{+/-}$ mice, respectively). This corroborates our morphological analyses in that the decreased functional recovery in the $HKII^{+/-}$ mice is probably mostly the result of the increased initial damage and not of a slower rate of recovery during the 14 days of healing. Because the force measurements are normalized to muscle mass, the diminished force production in the reperfused muscles indicates that the regenerating, centronucleated fibers are still in the immature state after 14 days of recovery and not yet fully integrated as functional muscle units.

The increase in fatigue resistance measured after I/R correlates with other reports (2, 37) and possibly reflects a transition of muscle fiber type from fast-twitch to slow oxidative fibers (2, 36). GM muscle predominantly consists of fast-twitch fibers (4), which are relatively prone to fatigue (36). The proposed change to a more fatigue-resistant fiber type due to I/R would therefore reduce fatigue vulnerability. Besides a switch in fiber type, increased fatigue resistance may also be explained by the I/R-induced increase in HK activity, as observed in the present study. Fueger and colleagues have shown in different studies that the HKII protein content is a determinant of endurance capacity (15). Additionally, during exercise muscle glucose uptake is reduced in HKII-reduced animals (13), while the glucose transporter GLUT4 is unaffected by HKII reduction (14), making glucose phosphorylation a limiting factor for muscle glucose uptake (12, 13). Therefore, glucose phosphorylation by HK is a limiting factor for muscle endurance and fatigue properties, and the increase in HK activity observed in the reperfused muscles of both genotypes may partly explain the increased fatigue resistance.

In summary, our results demonstrate that reduced HKII protein content results in impaired muscle functionality at 14 day recovery following an I/R episode. The impaired recovery seems to be mainly a result of a greater susceptibility of $HKII^{+/-}$ mice to I/R-induced acute necrosis (not apoptosis) and is not related to a HKII-related deficiency in muscle regeneration. The data suggest that manipulation of HKII protein content before I/R interventions may be a promising avenue for preventing muscle dysfunction following I/R.

GRANTS

This research was supported by Dutch Heart Foundation Grant No. NHS2010B011 (C. J. Zuurbier).

DISCLOSURES

No conflicts of interest, financial or otherwise, are declared by the author(s).

AUTHOR CONTRIBUTIONS

Author contributions: K.M.S., O.E., A.D.H., M.R.D., and C.J.Z. conception and design of research; K.M.S., O.E., A.K., R.B., J.K.N., and C.J.Z. performed experiments; K.M.S., G.S., R.B., J.K.N., R.N., M.B., and C.J.Z. analyzed data; K.M.S., O.E., G.S., R.B., J.K.N., C.I., A.D.H., M.R.D., and C.J.Z. interpreted results of experiments; K.M.S. and C.J.Z. prepared figures; K.M.S. drafted manuscript; K.M.S., O.E., G.S., A.K., R.B., J.K.N., C.I., R.N., M.B., M.L., A.D.H., M.R.D., M.W.H., and C.J.Z. approved final version of manuscript; O.E., R.B., A.D.H., M.R.D., M.W.H., and C.J.Z. edited and revised manuscript.

REFERENCES

1. **Antonsson B, Montessuit S, Sanchez B, Martinou JC.** Bax is present as a high molecular weight oligomer/complex in the mitochondrial membrane of apoptotic cells. *J Biol Chem* 276: 11615–11623, 2001.
2. **Awerbuck D, Luong V, Plyley MJ, McKee NH.** Skeletal muscle form and function after 4 hr ischemia-hypothermia. *J Surg Res* 57: 480–486, 1994.
3. **Bergmeyer HU, Bergmeyer J, Grassl M.** *Methods of Enzymatic Analysis*. Weinheim, Germany: VCH Verlagsgesellschaft, 1986.
4. **Blaisdell FW.** The pathophysiology of skeletal muscle ischemia and the reperfusion syndrome: a review. *Cardiovasc Surg* 10: 620–630, 2002.
5. **Chan RK, Austen WG, Ibrahim S, Ding GY, Verna N, Hechtman HB, Moore FD Jr.** Reperfusion injury to skeletal muscle affects primarily type II muscle fibers. *J Surg Res* 122: 54–60, 2004.
6. **Choi B, Kang NM, Nelson JS.** Laser speckle imaging for monitoring blood flow dynamics in the in vivo rodent dorsal skin fold model. *Microvasc Res* 68: 143–146, 2004.
7. **Crawford RS, Hashmi FF, Jones JE, Albadawi H, McCormack M, Eberlin K, Entabi F, Atkins MD, Conrad MF, Austen WG Jr, Watkins MT.** A novel model of acute murine hindlimb ischemia. *Am J Physiol Heart Circ Physiol* 292: H830–H837, 2007.
8. **Cross HR, Opie LH, Radda GK, Clarke K.** Is a high glycogen content beneficial or detrimental to the ischemic rat heart? A controversy resolved. *Circ Res* 78: 482–491, 1996.
9. **da-Silva WS, Gomez-Puyou A, de Gomez-Puyou MT, Moreno-Sanchez R, De Felice FG, de ML, Oliveira MF, Galina A.** Mitochondrial bound hexokinase activity as a preventive antioxidant defense: steady-state ADP formation as a regulatory mechanism of membrane potential and reactive oxygen species generation in mitochondria. *J Biol Chem* 279: 39846–39855, 2004.
10. **Eerbeek O, Kernell D, Verhey BA.** Effects of fast and slow patterns of tonic long-term stimulation on contractile properties of fast muscle in the cat. *J Physiol* 352: 73–90, 1984.
11. **Forrester KR, Stewart C, Tulip J, Leonard C, Bray RC.** Comparison of laser speckle and laser Doppler perfusion imaging: measurement in human skin and rabbit articular tissue. *Med Biol Eng Comput* 40: 687–697, 2002.
12. **Fueger PT, Bracy DP, Malabanan CM, Pencek RR, Wasserman DH.** Distributed control of glucose uptake by working muscles of conscious mice: roles of transport and phosphorylation. *Am J Physiol Endocrinol Metab* 286: E77–E84, 2004.

13. **Fueger PT, Heikkinen S, Bracy DP, Malabanan CM, Pencek RR, Laakso M, Wasserman DH.** Hexokinase II partial knockout impairs exercise-stimulated glucose uptake in oxidative muscles of mice. *Am J Physiol Endocrinol Metab* 285: E958–E963, 2003.
14. **Fueger PT, Lee-Young RS, Shearer J, Bracy DP, Heikkinen S, Laakso M, Rottman JN, Wasserman DH.** Phosphorylation barriers to skeletal and cardiac muscle glucose uptakes in high-fat fed mice: studies in mice with a 50% reduction of hexokinase II. *Diabetes* 56: 2476–2484, 2007.
15. **Fueger PT, Shearer J, Krueger TM, Posey KA, Bracy DP, Heikkinen S, Laakso M, Rottman JN, Wasserman DH.** Hexokinase II protein content is a determinant of exercise endurance capacity in the mouse. *J Physiol* 566: 533–541, 2005.
16. **Gürel E, Smeele KM, Eerbeek O, Koeman A, Demirci C, Hollmann MW, Zuurbier CJ.** Ischemic preconditioning affects hexokinase activity and HKII in different subcellular compartments throughout cardiac ischemia-reperfusion. *J Appl Physiol* 106: 1909–1916, 2009.
17. **Heikkinen S, Pietila M, Halmekyto M, Suppola S, Pirinen E, Deeb SS, Janne J, Laakso M.** Hexokinase II-deficient mice. Prenatal death of homozygotes without disturbances in glucose tolerance in heterozygotes. *J Biol Chem* 274: 22517–22523, 1999.
18. **Johnson C, Sung HK, Lessner SM, Fini ME, Galis ZS.** Matrix metalloproteinase-9 is required for adequate angiogenic revascularization of ischemic tissues. Potential role in capillary branching. *Circ Res* 94: 262–268, 2004.
19. **Kan HE, Buse-Pot TE, Peco R, Isbrandt D, Heerschap A, de Haan A.** Lower force and impaired performance during high-intensity electrical stimulation in skeletal muscle of GAMT-deficient knockout mice. *Am J Physiol Cell Physiol* 289: C113–C119, 2005.
20. **Kang J, Albadawi H, Patel VI, Abbruzzese TA, Yoo JH, Austen WG Jr, Watkins MT.** Apolipoprotein E−/− mice have delayed skeletal muscle healing after hind limb ischemia-reperfusion. *J Vasc Surg* 48: 701–708, 2008.
21. **Katzen HM, Soderman DD, Wiley CE.** Multiple forms of hexokinase. Activities associated with subcellular particulate and soluble fractions of normal and streptozotocin diabetic rat tissues. *J Biol Chem* 245: 4081–4096, 1970.
22. **Kung G, Konstantinidis K, Kitsis RN.** Programmed necrosis, not apoptosis, in the heart. *Circ Res* 108: 1017–1036, 2011.
23. **Lyon AR, Joudrey PJ, Jin D, Nass RD, Aon MA, O'Rourke B, Akar FG.** Optical imaging of mitochondrial function uncovers actively propagating waves of mitochondrial membrane potential collapse across intact heart. *J Mol Cell Cardiol* 49: 565–575, 2010.
24. **Majewski N, Nogueira V, Bhaskar P, Coy PE, Skeen JE, Gottlob K, Chandel NS, Thompson CB, Robey RB, Hay N.** Hexokinase-mitochondria interaction mediated by Akt is required to inhibit apoptosis in the presence or absence of Bax and Bak. *Mol Cell* 16: 819–830, 2004.
25. **Mathupala SP, Ko YH, Pedersen PL.** Hexokinase-2 bound to mitochondria: cancer's Stygian link to the "Warburg Effect" and a pivotal target for effective therapy. *Semin Cancer Biol* 19: 17–24, 2009.
26. **McCormack MC, Kwon E, Eberlin KR, Randolph M, Friend DS, Thomas AC, Watkins MT, Austen WG Jr.** Development of reproducible histologic injury severity scores: skeletal muscle reperfusion injury. *Surgery* 143: 126–133, 2008.
27. **Paoni NF, Peale F, Wang F, Errett-Baroncini C, Steinmetz H, Toy K, Bai W, Williams PM, Bunting S, Gerritsen ME, Powell-Braxton L.** Time course of skeletal muscle repair and gene expression following acute hind limb ischemia in mice. *Physiol Genomics* 11: 263–272, 2002.
28. **Pasdois P, Parker JE, Griffiths EJ, Halestrap A.** The role of oxidized cytochrome c in regulating mitochondrial reactive oxygen species production and its perturbation in ischaemia. *Biochem J* 436: 493–505, 2011.
29. **Pastorino JG, Shulga N, Hoek JB.** Mitochondrial binding of hexokinase II inhibits Bax-induced cytochrome c release and apoptosis. *J Biol Chem* 277: 7610–7618, 2002.
30. **Robey RB, Hay N.** Mitochondrial hexokinases: guardians of the mitochondria. *Cell Cycle* 4: 654–658, 2005.
31. **Rostovtseva TK, Tan W, Colombini M.** On the role of VDAC in apoptosis: fact and fiction. *J Bioenerg Biomembr* 37: 129–142, 2005.
32. **Smeele KM, Eerbeek O, Koeman A, Bezemer R, Ince C, Heikkinen S, Laakso M, de Haan A, Schaart G, Drost MR, Hollmann MW, Zuurbier CJ.** Partial hexokinase II knockout results in acute ischemia-reperfusion damage in skeletal muscle of male, but not female, mice. *Pflügers Arch* 459: 705–712, 2010.
33. **Smeele KM, Southworth R, Wu R, Xie C, Nederlof R, Warley A, Nelson JK, van HP, van den Wijngaard JP, Heikkinen S, Laakso M, Koeman A, Siebes M, Eerbeek O, Akar FG, Ardehali H, Hollmann MW, Zuurbier CJ.** Disruption of hexokinase II-mitochondrial binding blocks ischemic preconditioning and causes rapid cardiac necrosis. *Circ Res* 108: 1165–1169, 2011.
34. **Smeele KM, Ter Horst LH, Koeman A, Heikkinen S, Laakso M, Weber NC, Hollmann MW, Zuurbier CJ.** The effect of standard chow and reduced hexokinase II on growth, cardiac and skeletal muscle hexokinase and low-flow cardiac ischaemia-reperfusion injury. *Lab Anim* 45: 160–166, 2011.
35. **Vignaud A, Hourde C, Medja F, Agbulut O, Butler-Browne G, Ferry A.** Impaired skeletal muscle repair after ischemia-reperfusion injury in mice. *J Biomed Biotechnol* 2010: 724914, 2010.
36. **Westerblad H, Bruton JD, Katz A.** Skeletal muscle: energy metabolism, fiber types, fatigue and adaptability. *Exp Cell Res* 316: 3093–3099, 2010.
37. **Woitaske MD, McCarter RJ.** Effects of fiber type on ischemia-reperfusion injury in mouse skeletal muscle. *Plast Reconstr Surg* 102: 2052–2063, 1998.
38. **Wu R, Smeele KM, Wyatt E, Ichikawa Y, Eerbeek O, Sun L, Chawla K, Hollmann MW, Nagpal V, Heikkinen S, Laakso M, Jujo K, Wasserstrom JA, Zuurbier CJ, Ardehali H.** Reduction in hexokinase II levels results in decreased cardiac function and altered remodeling after ischemia/reperfusion injury. *Circ Res* 108: 60–69, 2011.
39. **Zheng J, Wang R, Zambraski E, Wu D, Jacobson KA, Liang BT.** Protective roles of adenosine A1, A2A, and A3 receptors in skeletal muscle ischemia and reperfusion injury. *Am J Physiol Heart Circ Physiol* 293: H3685–H3691, 2007.
40. **Zuurbier CJ, Smeele KMA, Eerbeek O.** Mitochondrial hexokinase and cardioprotection of the intact heart. *J Bioenerg Biomembr* 41: 181–185, 2009.
41. **Zuurbier CJ, Emons VM, Ince C.** Hemodynamics of anesthetized ventilated mouse models: aspects of anesthetics, fluid support, and strain. *Am J Physiol Heart Circ Physiol* 282: H2099–H2105, 2002.
42. **Zuurbier CJ, Huijing PA.** Influence of muscle shortening on the geometry of gastrocnemius medialis muscle of the rat. *Acta Anat (Basel)* 140: 297–303, 1991.